Journal of Electroceramics, 11, 81–87, 2003

Varistors Based on Doped SnO_2

SANJAY R. DHAGE,[1] VIOLET SAMUEL[2] & V. RAVI[1,*]
[1] *Physical and Materials Chemistry Division, National Chemical Laboratory, Pune-411008, India*
[2] *Catalysis Division, National Chemical Laboratory, Pune-411008, India*

Submitted August 4, 2003; Revised November 3, 2003; Accepted November 4, 2003

Abstract. When tin oxide is doped with either Sb_2O_3 and CoO or Ta_2O_5 and CoO, it shows highly nonlinear current (I)–voltage (V) characteristics. Addition of CoO leads to creation of oxygen vacancies and helps in sintering of SnO_2. Both tantalum and antimony act as donors and increases the conductivity. The change in nonlinear coefficient (α) and the breakdown voltage (E_B) are studied as function of the quantity of the donor introduced. The magnitudes of grain size and grain boundary barrier height (Φ_B) are calculated as a function of duration of sintering. The observed nonlinear coefficient (α) is in the range of 3–34 and the breakdown voltage varies from 110 V/cm to 4400 V/cm. Incorporation of 5 mole% titanium leads to increase in both α and E_B values. All the samples show single phase as found by X-ray diffraction. These samples exhibit low breakdown voltages as compared to commercial ZnO varistors.

Keywords: varistor, SnO_2, Schottky barrier

1. Introduction

Varistors (voltage dependent resistors) based on polycrystalline ZnO ceramics are already commercially available to protect electrical/electronic components from transient overvoltages [1, 2]. The important parameters that characterize a typical varistor are nonlinear coefficient (α), breakdown voltage and energy absorption. The advantage of ZnO varistor is their energy absorption capability when compared to conventional Zener diodes. However, the breakdown voltage is very high (3.2 V per grain boundary) and precludes them for low voltage applications [1, 2]. Various techniques to grow larger grain sizes such as seed method have been adopted to overcome this drawback [3]. Simultaneously the search for varistor action in other systems has led to discovery nonlinear I-V characteristics in TiO_2 [4], $SrTiO_3$ [5] and SnO_2 [6–12]. However the α values are not as high as found in ZnO ceramics ($\alpha = 50 - 75$). The present investigations focus our efforts to develop varistor based on doped SnO_2. Tin oxide is an *n*-type semiconductor with many interesting electronic properties. Tin oxide with ∼1 mole% antimony oxide exhibits quasi-metallic conductivity while maintaining transparency in the optical region [13]. This optoelectronic property is exploited in optical devices and solar cells. At higher concentration of antimony oxide, the conductivity decreases due to charge compensation occurring by multiple valency of antimony oxide i.e. due to presence of Sb^{3+} ion conductivity decreases [14]. Thin film of tin doped indium oxide is a degenerate wide band gap semiconducting oxide, which is commonly used in optoelectronic applications that require a transparent electrode with high optical transmissivity of visible light and reasonable conductivity [13]. The other major application is its property of gas sensing asises due to its poor sinterability in air in pure form even at high temperatures [9]. The aim of the present work is to study the nonlinear I-V characteristics of doped tin oxide ceramics.

*To whom all correspondence should be addressed. E-mail: ravi@ems.ncl.res.in

2. Experimental Procedure

SnO_2 containing additives was prepared by the standard ceramic technique. The SnO_2, along with dopants such as CoO and Sb_2O_5 or Ta_2O_5 in the stoichiometric ratio

Table 1. Characteristics of (99-X)% SnO_2 + 1% CoO + X% Sb_2O_3/Ta_2O_5 (SCA and SCTa series)

	Sintering time: 4 hr						Sintering time: 24 hr					
	α	E_B (V cm^{-1})	Density (g cm^{-3})	Relative density (%)	Φ_B (eV)	Average grain size (μm)	α	E_B (V cm^{-1})	Density (g cm^{-3})	Relative density (%)	Φ_B (eV)	Average grain size (μm)
$X = Sb_2O_3$												
0.01	19	1325	6.50	93.5	0.424	4	12	375	6.42	92.3	0.339	6
0.05	14	725	6.58	94.7	0.377	4	8	220	6.35	91.4	0.299	5
0.1	9	435	6.37	91.7	0.309	5	9	390	6.40	92.1	0.344	4
0.5	3	110	6.35	91.4	0.242	6	C[a]	–	6.28	94.5	–	8
$X = Ta_2O_5$												
0.01	21	1250	6.68	96.1	0.448	2	12	520	6.64	95.5	0.356	4
0.05	18	1270	6.60	94.9	0.414	2	13	780	6.71	96.5	0.362	3
0.1	18	1365	6.65	95.7	0.413	2	13	745	6.71	96.5	0.358	3
0.5	36	4925	6.73	96.8	0.627	2	16	1095	6.68	91.1	0.389	4

d_t Single crystal density of tetragonal rutile SnO_2 is 6.95 g cm^{-3}.
[a]Conducting.

Table 2. Characteristics of (94-X)% SnO_2 + 5% TiO_2 + 1% CoO + X% Sb_2O_3/Ta_2O_5 (STCA and STCTa series)

	Sintering time: 4 hr						Sintering time: 24 hr					
	α	E_B (V cm^{-1})	Density (g cm^{-3})	Relative density (%)	Φ_B (eV)	Average grain size (μm)	α	E_B (V cm^{-1})	Density (g cm^{-3})	Relative density (%)	Φ_B (eV)	Average grain size (μm)
$X = Sb_2O_3$												
0.01	26	2540	6.67	96.0	0.498	6	20	1570	6.47	93.1	0.434	10
0.05	24	1960	6.47	93.1	0.460	7	19	1015	6.45	92.8	0.433	9
0.1	20	1620	6.41	92.2	0.436	7	16	940	6.68	96.1	0.393	10
0.5	17	1930	6.42	92.4	0.400	8	14	860	6.47	93.1	0.368	9
$X = Ta_2O_5$												
0.01	32	3600	6.35	91.3	0.569	5	26	2245	6.61	95.1	0.469	10
0.05	28	2740	6.40	91.1	0.526	6	24	1400	6.56	94.4	0.469	9
0.1	27	2880	6.40	92.1	0.516	6	24	1615	6.69	96.2	0.478	9
0.5	I[a]	–	6.26	90.1	–	4	34	4350	6.58	94.7	0.597	10

[a]Insulating.

were mixed and ground well and calcined at 1473 K for 24 hrs. The calcined powders were again ground and fired at 1473 K for another 24 hrs. Two series of compositions are prepared with respect to each donor as given below. 5 mole% of TiO_2 is substituted for SnO_2 in each case to study the influence of it. The molar compositions are; Serie-(SCA) (99-X)% SnO_2 + 1% CoO + X%Sb_2O_3, Serie-(STCA) (94-X)% SnO_2 + 5% TiO_2 + 1% CoO + X%Sb_2O_3, Serie-(SCTa) (99-X)% SnO_2 + 1% CoO + X% Ta_2O_5 and Serie-(STCTa) (94-X)% SnO_2 + 5% TiO_2 + 1% CoO + X% Ta_2O_5, where $x = 0.01, 0.05, 0.1$ and 0.5 at%. The calcined powders were mixed with a binder (poly vinyl alcohol 2 wt%) and pelletized (15 mm dia, 1 mm thick) at 2–3 tons. The pellets were sintered at 1573 K for different durations ranging from 4 to 24 hrs. The values of various parameters for the above compositions are given in Tables 1 and 2. The sintered pellets were polished and ohmic silver contacts were obtained by curing Ag-paste and annealed at 873 K for 30 minutes.

The structure related phase determination was studied by Philip 1730 X-ray diffractometer. The microstructure of the sintered pellets was observed using a Leica Cambridge 440 microscope. The I-V

characteristics were measured by using Kiethley electrometer 6517A, high resistance meter. It also contains a built in one-kilovolt dc power supply so that there is no need of external power supply in the circuit. The Current-Voltage relation of a varistor is given by the equation,

$$J = (E/C)^{\alpha} \tag{1}$$

where J is the current density, E is the applied field, C the proportionality constant and α is the nonlinear coefficient. The current-voltage curves were plotted on log–log scale from which the slope of the curve gives the value of α. The important parameter, E_B breakdown voltage is taken as the field applied when current flowing through the varistor is 1 mA. Since Schottky type grain boundary barriers are present in the present samples the current density in ohmic region of varistor is related to the electric field and the temperature given by Eq. (2)

$$J = \mathrm{AT}^2 \exp[(\beta E^{1/2} - \Phi_B)/kT] \tag{2}$$

Where A, equal to $4\rho \mathrm{emk}^2/\mathrm{h}^3$, is Richardson's constant, ρ is the bulk density of SnO_2, e is electron charge, m is electron mass, k is Boltzmann constant, h is plank constant, Φ_B is interface barrier height, and β is constant related to the relationship

$$\beta\alpha 1/(r\omega) \tag{3}$$

where 'r' is grain number per unit length and ω is the barrier width. Measuring the current density in ohmic region and keeping the temperature of the tested varistor constant, for two different applied fields the equations are,

$$J_1 = \mathrm{AT}^2 \exp\left[\left(\beta E_1^{1/2} - \Phi_B\right)/kT\right] \tag{4}$$

$$J_2 = \mathrm{AT}^2 \exp\left[\left(\beta E_2^{1/2} - \Phi_B\right)/kT\right] \tag{5}$$

The values of Φ_B and β can be calculated from above equations.

3. Results and Discussion

Figure 1 shows the X-ray diffractogram (XRD) recorded for the samples with and without TiO_2. No second phases are found and all the lines are corresponding to SnO_2 tetragonal rutile type phase. It is also

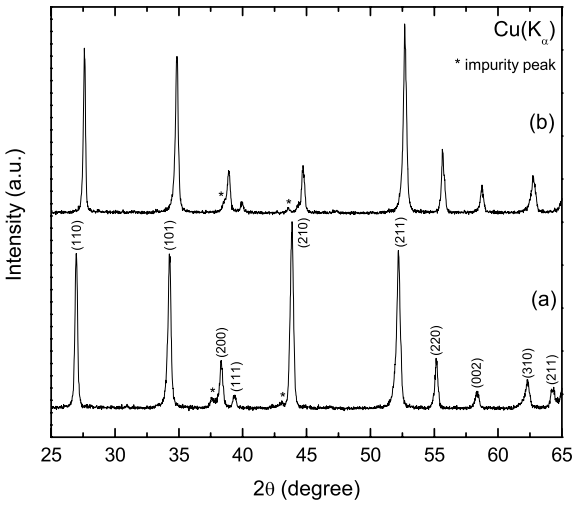

Fig. 1. XRD of sintered SnO_2 containing (a) SCA and (b) STCA at room temperature.

to be noted that the concentrations of dopants added are too small to be detected by X-rays. The calculated lattice parameters by least square fit for the samples with 5 mole% TiO_2 are $a = 0.4651$ nm and $c = 0.3151$ nm (for samples without TiO_2 $a = 0.4695$ nm and $c = 0.3166$ nm). Both the cell parameter of the tetragonal rutile structure of SnO_2 decrease by incorporation of TiO_2 this is accordance with decrease in ionic radius as Sn^{4+} (0.071 nm) is substituted by isovalent Ti^{4+} (0.068 nm)[6]. The density of all the sintered samples varies from 91 to 97% of the single crystal values (Tables 1 and 2). The I-V characteristics for samples sintered at 1573 K for 4 hr and 24 hrs of the systems SCA, SCTa, STCA, STCTa are illustrated in Figs. 2–5. Thecorresponding values of α, Φ_B and E_B are tabulated in Tables 1 and 2. The Table also shows the effect of sintering duration on the electrical properties. The α values for the antimony doped samples vary from 19 to 3 depending on content of antimony as shown in Fig. 2. The breakdown field strength decreases with the decrease in α values. From Fig. 3, one can observe that the highest α value (=36) is obtained for tantalum doped samples. The breakdown field strength is also correspondingly high for this Serie. The influence of addition of 5 mol% titanium on the I-V curves can be seen in Figs. 4 and 5 for the antimony and tantalum doped samples respectively. The microstructures of these typical sintered samples are shown in Fig. 6. The grain size varies from 2 to 10 μm depending on the duration of sintering. The average grain size increases

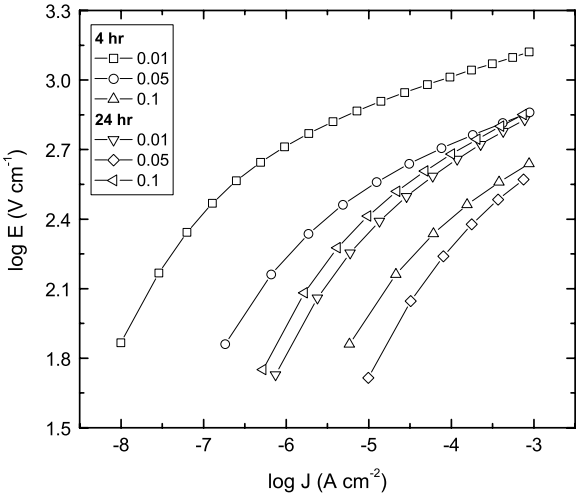

Fig. 2. I-V characteristics of Series-SCA (99-X)% SnO_2 + 1% CoO + X% Sb_2O_3.

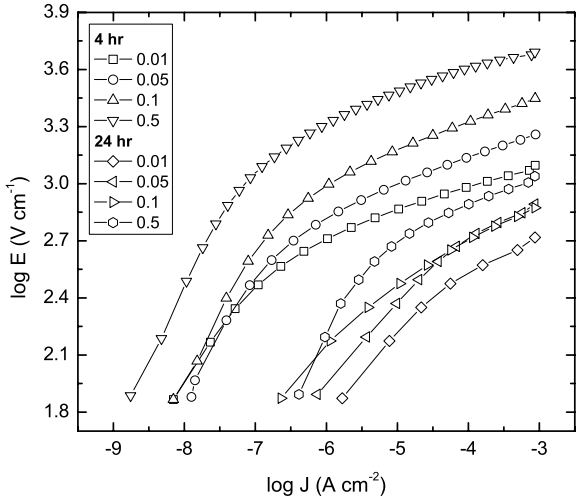

Fig. 3. I-V characteristics of Series-SCTa (99-X)% SnO_2 + 1% CoO + X% Ta_2O_5.

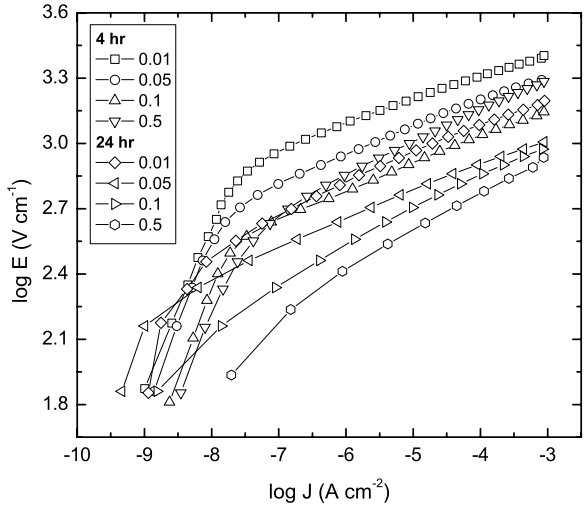

Fig. 4. I-V characteristics of Series-STCA (94-X)% SnO_2 + 5% TiO_2 + 1% CoO + X% Sb_2O_3.

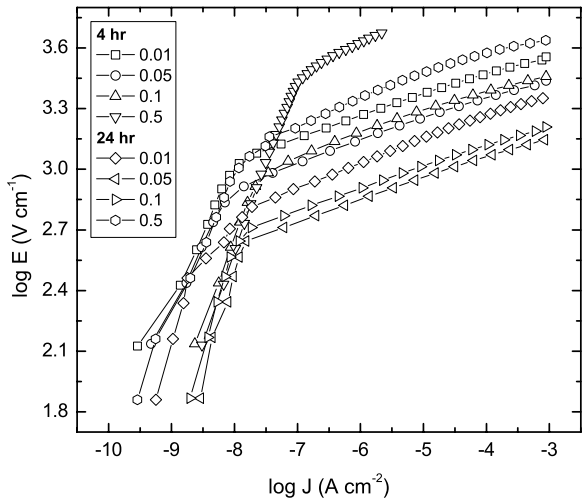

Fig. 5. I-V characteristics of Series-STCTa (94-X)% SnO_2 + 5% TiO_2 + 1% CoO + X% Ta_2O_5.

with increase in the duration of sintering. The grain size also increases with incorporation of 5 mol% titanium in the samples (see Tables 1 and 2). No porosity is found indicating good densification of the samples. No secondary phases are found at grain boundaries or at triple points.

3.1. Antimony Doped Samples

When the content of antimony is between 0.1 and 0.5 at%, the room temperature resistivity decreases tremendously [16] and the samples behave as good conductors at high concentrations of antimony, particularly when sintering duration is long (see Table 1). Low voltage varistors are realized, for the duration of sintering is >12 h at 1573 K (The corresponding $\alpha = 3$, $E_B = 110$ V/cm and $\Phi_B = 0.242$ eV). However as mentioned, the α values are low for this case. The decrease in breakdown voltage with increase in the duration of sintering is due to grain growth that occurs in these ceramics. When 5 mole% of titanium

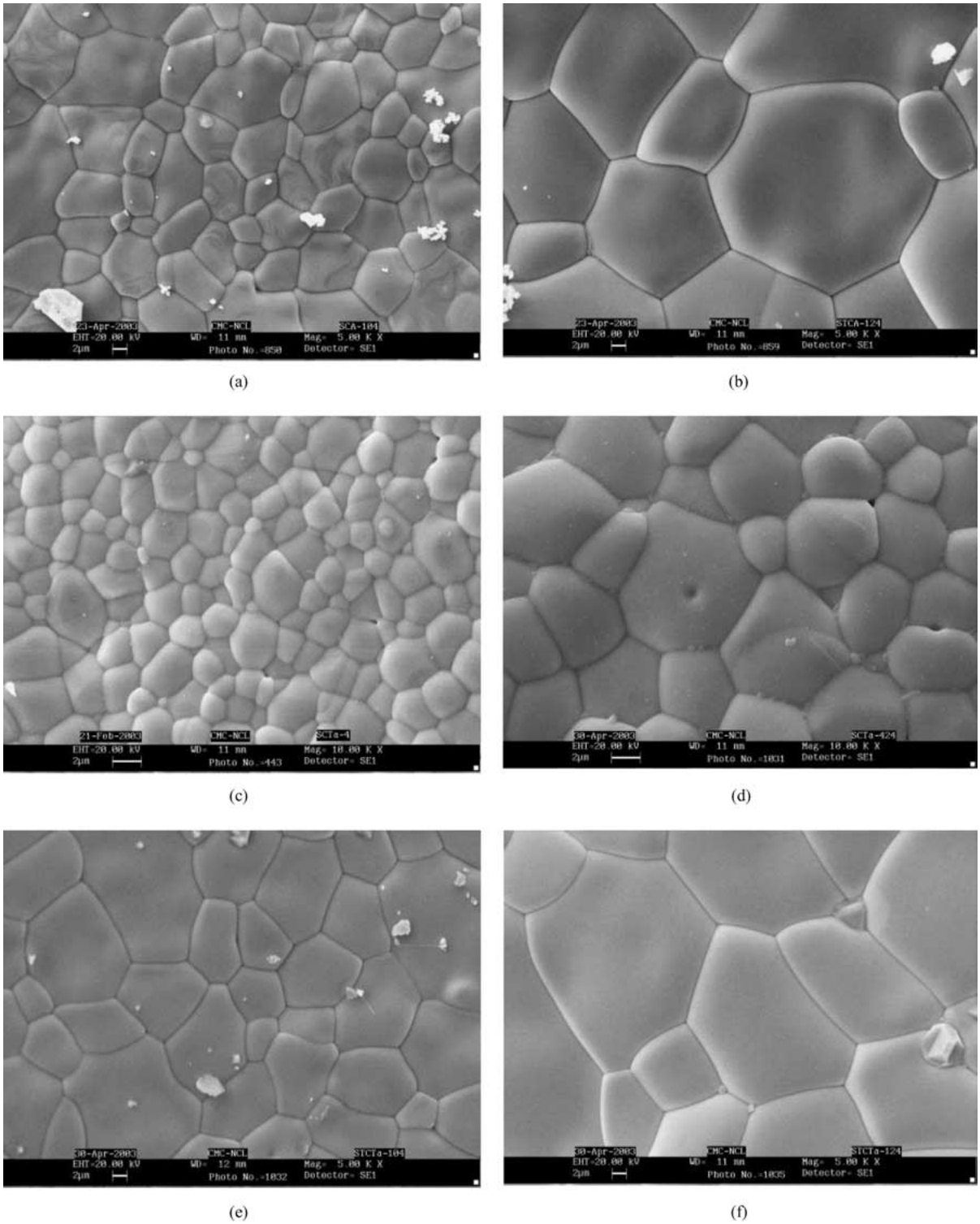

Fig. 6. Microstructure of various SnO_2 systems sintered at 1300 for (a) SCA-0.05 (Sb) 4 hr, (b) STCA-0.05 (Sb) 24 hr, (c) SCTa-0.5 (Ta) 4 hr, (d) SCTa-0.5 (Ta) 24 hr, (e) STCTa-0.01 (Ta) 4 hr, (f) STCTa-0.01 (Ta) 24 hr.

is introduced, both α and E_B increase. For antimony doped samples, the α value increases from 19 to 26 with titanium addition as shown in Tables 1 and 2. The corresponding breakdown field strength also goes up from 1325 to 2540 V/cm. The same trend is observed for tantalum-doped samples. The introduced titanium ion goes into lattice as shown by decrease in the lattice parameters. It is not clear until now why incorporation of titanium increases these functional parameters and interaction between antimony and titanium may be one reason that leads to high α and E_B values.

3.2. Tantalum Doped Samples

Tables 1 and 2 show the results of various amounts of tantalum doped tin oxide samples. The values of α, Φ_B and E_B are correspondingly high when compared to antimony doped samples. In contrast to antimony-doped samples the conductivity does not increase with increase in the tantalum concentration as shown in the Tables 1 and 2. The incorporation of tantalum is probably charge compensated by electrons at lower concentrations (Eq. (10)) and by cation vacancies at higher concentrations [16] as shown by above results. This may be further complicated in the case of antimony doped samples by the presence of both Sb^{5+} and Sb^{3+} ions (Eqs. (11) and (12)). It is also to be noted that the values of breakdown voltages obtained are much smaller than that reported for commercial ZnO varistors [1, 2].

The varistor action observed in polycrystalline ZnO ceramics is explained by the presence of Schottky type energy barrier at the grain boundaries. In the present case the acceptor like surface states formed by CoO will lead to formation of energy barrier at the grain boundaries, which is here rather small. This is unlike other tin oxide system reported by us [7] recently, wherein the presence of rare earth ion at the grain boundaries leads to formation grain boundary defect states. There the ionic radius of La^{3+} ion being larger than Sn^{4+} ion, it prefers grain boundary site. This modification resulted in relatively better α values. As mentioned in the introduction the addition of small quantities of transition metal oxides such as CoO to tin oxide helps in its densification [12]. For example with 1 mol% CoO, the sinter density is >94% when sintered at 1573 K for one hour. The Co^{2+} ion having lower valence creates oxygen vacancies in tin oxide lattice, which is rate determining step for sintering. At low temperature the CoO may take up oxygen and at high temperatures CoO is the stable phase releasing oxygen to its environment as given below

$$2CoO + \tfrac{1}{2}O_2 \overset{773-953\,K}{\rightarrow} Co_2O_3 \quad (6)$$

$$Co_2O_3 \overset{1223\,K}{\rightarrow} 2CoO + \tfrac{1}{2}O_2 \quad (7)$$

The densification of tin oxide ceramics has been attributed [12] to the effect of cobalt in the SnO_2 lattice, which leads to the formation of oxygen vacancies according to the following equations,

$$CoO \overset{SnO_2}{\rightarrow} Co''_{Sn} + V^{\bullet\bullet}_{o} + O^{x}_{o} \quad (8)$$

$$Co_2O_3 \overset{SnO_2}{\rightarrow} 2Co'_{Sn} + V^{\bullet}_{o} + O^{x}_{o} \quad (9)$$

Small amount of Ta_2O_5 were added to SnO_2 ceramics to promote the substitution of Sn^{4+} for Ta^{5+} leading to an increase of electronic conductivity in the SnO_2 lattice [16] according to,

$$Ta_2O_5 \overset{SnO_2}{\rightarrow} 2Ta^{\bullet}_{Sn} + 2e' + 4O^{x}_{o} + \tfrac{1}{2}O_2 \quad (10)$$

Sb_2O_5 is the stable form up to 1243 K, but Sb_2O_3 is more stable higher temperature, however the Sb^{5+}/Sb^{3+} ratio will depend both on the temperature and on the concentration at ambient oxygen [15] then it is possible that during the cooling process the transformation of Sb^{3+} into Sb^{5+} takes place. At lower concentrations Antimony present as pentavalent and acts as donor. The defect reactions may be given as

$$Sb_2O_3 \overset{SnO_2}{\rightarrow} 2Sb'_{Sn} + V^{\bullet\bullet}_{o} + 3O^{x}_{o} \quad (11)$$

$$Sb_2O_5 \overset{SnO_2}{\rightarrow} 2Sb^{\bullet}_{Sn} + 2e' + 4O^{x}_{o} + \tfrac{1}{2}O_2 \quad (12)$$

A schematic grain boundary barrier diagram modified from [11] is shown in Fig. 7 wherein possible negative surface states are also given. In the present case no additional element like Cr [11] is present at the grain boundaries. The defects are generated due to aliovalent ions like Co and Sb doping in tin dioxide ceramics. It is to be noted that no segregation of impurity at grain boundary is expected since all the above ions will go into lattice. The calculated values of barrier height are lower than that reported for ZnO varistors [1, 2].

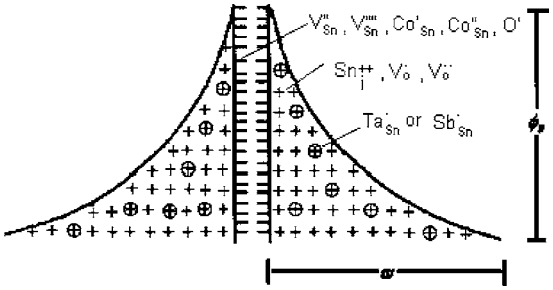

Fig. 7. Schematic diagram of Schottky type grain boundary barrier.

4. Conclusions

Tin oxide shows nonlinear I-V characteristics when doped with small quantities of CoO, and Sb_2O_5 or Ta_2O_5. The nonlinear coefficient values are dependent both composition and processing parameters. Under optimum conditions i.e. at longer durations of sintering low voltage varistors are realized. Addition of 5 mole% TiO_2 improves the nonlinear current—voltage characteristics. The present varistor system contains less number of additives when compared to commercial ZnO ceramics wherein a variety of metal oxides are added in small quantities to achieve optimum properties.

Acknowledgment

We are thankful to CMC (Center for Materials Characterization) for instrumental facility. The project has been funded by Department of Science and Technology (DST) Govt. of India (grant no. Sp/S1/ H-19/ 2000).

References

1. D.R. Clarke, *J. Am. Ceram. Soc.*, **82**, 485 (1999).
2. T.K. Gupta, *J. Am. Ceram. Soc.*, **73**, 1817 (1990).
3. X. Quing, Chen Wen, and Y. Run-Zhang, *Transaction of Nonferrous Metals Society of China*, **11**, 328 (2001).
4. M.F. Yan and W.W. Rhodes, *Appl. Phy. Lett.*, **40**, 536 (1982).
5. M. Fujimoto, Y.M. Chiang, A. Roshko, and W.D. Kingery, *J. Am. Ceram. Soc.*, **68**, C300 (1985).
6. V. Ravi and S.K. Date, *Bull. Mater. Sci.*, **24**, 483 (2001).
7. S.R. Dhage, V. Ravi, and S.K. Date, *Mater. Lett.*, **57**, 727 (2002).
8. P.N. Santhosh, H.S. Potadar, and S.K. Date, *J. Mater. Res.*, **12**, 326 (1997).
9. S.A. Pianaro, P.R. Bueno, E. Longo, and J.A. Varela, *J. Mater. Sci. Lett.*, **14**, 692 (1995).
10. P.R. Bueno, E.R. Leite, M.M. Oliveria, M.O. Orlandi, and E. Longo, *Appl. Phys. Lett.*, **79**, 48 (2001).
11. P.R. Bueno, S.A. Pianaro, E.C. Pereira, L.O. Bulhoes, E. Longo, and J.A. Varela, *J. Appl. Phys.*, **87**, 3700 (1998).
12. J.A. Cerri, E.R. Leite, D. Goueva, and E. Longo, *J. Amer. Ceram. Soc.*, **79**, 804 (1996).
13. C.W.O. Yang, D. Spinner, Y. Shigesato, and D.C. Paine, *J. Appl. Phys.*, **83**, 145 (1998).
14. K.C. Mishra, K.M. Johnson, and P.C. Schmidt, *Phy. Rev.*, B **51**, 13972 (1995).
15. A. Ovenston, D. Sprinceana, J.R. Walls, and M. Caldararu, *J. Mater. Sci.*, **29**, 4946 (1994).
16. S.R. Dhage and V. Ravi, *Appl. Phys. Lett.*, **83**, 4539 (2003).